Eur. Phys. J. A **39**, 349–363 (2009)
DOI 10.1140/epja/i2008-10717-0

THE EUROPEAN PHYSICAL JOURNAL A

Regular Article – Theoretical Physics

Pion mass shift and the kinetic freeze-out process

S. Zschocke[1,a] and L.P. Csernai[1,2]

[1] Section for Theoretical and Computational Physics, and Bergen Computational Physics Laboratory, University of Bergen, 5007 Bergen, Norway
[2] MTA-KFKI, Research Institute of Particle and Nuclear Physics, 1525 Budapest 114, Hungary

Received: 15 September 2008 / Revised: 22 December 2008
Published online: 11 February 2009 –
Communicated by T. Bíró

Abstract. The kinetic freeze-out process of a pion gas through a finite layer with time-like normal is considered. The pion gas is described by a Boltzmann gas with elastic collisions among the pions. Within this model, the impact of the in-medium pion mass modification on the freeze-out process is studied. A marginal change of the freeze-out variables temperature and flow velocity and an insignificant modification of the frozen-out particle distribution function has been found.

PACS. 24.10.Nz Hydrodynamic models – 25.75.-q Relativistic heavy-ion collisions

1 Introduction

One of the greatest discoveries in ultra-relativistic heavy-ion physics has been the creation of the Quark Gluon Plasma (QGP) at Super Proton Synchrotron (SPS) at Conseil Européen pour la Recherche Nucléaire (CERN) in 2000 [1] and at the Relativistic Heavy-Ion Collider (RHIC) at Brookhaven National Laboratory (BNL) in 2005 [2]. In fact, there are compelling experimental signatures which transformed the QGP from a theoretical prediction into a precise observational science: elliptic flow v_2, jet quenching, strangeness enhancement and constituent quark number scaling can hardly be understood without the clear statement that this new state of matter has been achieved. However, during the last years it turned out that the produced new state of matter is more similar to a strongly coupled or strongly interacting Quark Gluon Plasma (sQGP), which has more characteristics of a liquid than of a weakly interacting plasma of quarks and gluons [3–10]; for a recent comment on the term "sQGP" see [11]. While there is no doubt about a QGP phase transition of Quantum Chromodynamics (QCD) at $T_c = (173 \pm 8)$ MeV at vanishing baryonic densities [12], it seems that a QGP of freely moving partons can be reached only at higher energy densities and temperatures beyond the critical temperature T_c. These new insights imply that further experimental signatures are certainly needed to understand not only the physical features of sQGP, but also how the new experimental facts do coincide with the predictions of the fundamental theory of strong interactions. Further insights into this more complicated new state of matter are now expected from the intended experiments at the Large Hadron Collider (LHC) at CERN starting up very soon. In the following we will not distinguish between the terms QGP and sQGP, but want to keep in mind that the new state of matter is more complicated than expected from the early theoretical predictions.

The evidence of a QGP cannot be proven directly. Instead, we have to trace from the observables at the detectors back to this very early stage of the heavy-ion collision. Obviously, the more accurate the description of the subsequent processes after forming the QGP is, the more accurate will be the picture and the understanding of this new state of matter.

One promising theoretical method in this respect is the hydrodynamical approach based on the assumption of local thermal equilibrium. According to several theoretical studies, the produced QGP reaches a local thermal equilibrium very rapidly within (0.3–0.5) fm/c for gluons and (0.5–1.0) fm/c for the quarks [13–16]. Experimental data indicate a source size of less than 10 fm and less than 10 fm/c time extent. This strongly indicates a rapid pre-hadronization [17,18], which is also supported by the recent observation of constituent quark number scaling of collective flow data. Especially, when the expanding system reaches a temperature $T \leq T_c$ hadron states of high multiplicity, containing mostly pions, *e.g.* [19,20], are formed. The pre-thermalization of quarks and quark clusters or pre-hadrons results in the local thermalization of pions [21,22], and even most of the low-lying (s) hadronic states.

Subsequently after or even during the hadronization, the chemical and thermal Freeze-Out (FO) of the hadrons

[a] e-mail: sven.zschocke@tu-dresden.de

happens, where the hydrodynamical description breaks down and transport theoretical approaches are needed. First, the inelastic collisions among the hadrons cease, that is the so-called chemical FO at $T_{\rm ch}$. Immediately or simultaneously followed by the thermal FO at $T_{\rm th}$, where also the elastic collisions among the hadrons are abondened. The FO process is essentially the last stage of the heavy-ion collision process and the main source for observables. An accurate FO description is therefore a basis for an accurate understanding of the initial states produced in ultra-relativistic heavy-ion collisions.

A rigorous approach of the FO scenario from first principles is given by the Boltzmann transport equation which is a rather difficult assignment of a task. Even more, recently it has been recognized that the basic assumptions of the Boltzmann transport equation are spoiled at the last stages of the kinetic FO process [23,24], and a more involved modified Boltzmann transport equation has to be solved. The reason for that is because the characteristic lenght scale, describing the change of the distribution function, becomes smaller than the mean free path λ at the last stages of the kinetic FO process. Thus, phenomenological models which can describe the kinetic FO process in a simplified manner by taking into account the main features of a typical FO process only, become rather important.

Such a phenomenological description of the kinetic FO process is usually modeled by two different, in some sense even opposite, methods: a FO modeling through a hypersurface of zero thickness, and a FO modeling through an ininite space-time volume. Recently, the kinetic FO through a layer with finite thickness has been developed, for the case of the space-like normal in [25] and for the case of the time-like normal in [26]; see also [27,28]. This phenomenological approach makes a bridge between these mentioned two extreme FO models. So far, the impact of in-medium modifications of hadrons on the FO process has been considered only in refs. [29–31]. In our investigation we will apply this recently developed FO model and consider a kinetic FO scenario through a finite time-like layer to study the impact of in-medium pion mass modification on the FO process.

The paper is organized as follows: in sect. 2 we give the needed basics of a transport theoretical description of a hot and dense pion gas. The kinetic FO process through a finite time-like layer is considered in sect. 3. The finite-temperature mass modification of pions, embedded in a Boltzmann gas with elastic interactions among the pions, is examined in sect. 4. In sect. 5 we present the results obtained, and in sect. 6 a summary is given. Throughout the paper we take $c = \hbar = k_{\rm B} = 1$.

2 Transport theoretical description of a pion gas

Consider a system of N not necessarily conserved number of particles described by the one-particle distribution function $f(x,p)$. This invariant scalar function is normalized by $N = \int {\rm d}^3\boldsymbol{r}\, {\rm d}^3\boldsymbol{p}\, f(x,p)$. Throughout the paper we consider a dilute pion gas where only elastic scatterings among the pions are allowed, so that $x^\mu = (t, \boldsymbol{r})$ is the four-coordinate and $p^\mu = (p^0, \boldsymbol{p})$ is the four-momentum of the pion with $p^0 = \sqrt{m_\pi^2 + \boldsymbol{p}^2}$. Then, the particle four-flow is defined by, *e.g.* [32],

$$N^\mu = \int \frac{{\rm d}^3\boldsymbol{p}}{p^0}\, p^\mu\, f(x,p), \tag{1}$$

and the energy momentum tensor is

$$T^{\mu\nu} = \int \frac{{\rm d}^3\boldsymbol{p}}{p^0}\, p^\mu\, p^\nu\, f(x,p). \tag{2}$$

The four-flow velocity of the medium can be defined as a time-like unit tangent vector at the wordline of the particles, *i.e.* $u^\mu = \text{constant} \times N^\mu$ (Eckart's definition). However, in case of non-conserved particles like the pions are, such a definition would not be convinient. Instead, for non-conserved charges or non-conserved particles the four-flow velocity of the medium is usually defined as a time-like unit vector parallel to the energy flow, *i.e.* $u^\mu = \text{constant} \times T^{\mu\nu}\, u_\nu$ (Landau's definition):

$$u^\mu = \frac{T^{\mu\nu}\, u_\nu}{u_\rho\, T^{\rho\sigma}\, u_\sigma}\,. \tag{3}$$

This tensor equation (3) is by definition valid in any frame. Obviously, in the rest frame of the gas (RFG) we would have $u^\mu_{\rm RFG} = (1,0,0,0)$ in Eckart's as well as in Landau's definition of the four-flow velocity. Any other frame of interest is related to RFG just by a Lorentz boost.

From eq. (1) and eq. (2) one can define three linear independent Lorentz invariants: the scalar particle density n, the scalar energy density e and the scalar pressure P, given by

$$n = N^\mu\, u_\mu, \tag{4}$$

$$e = u_\mu\, T^{\mu\nu} u_\nu, \tag{5}$$

$$P = -\frac{1}{3} T^{\mu\nu}\, \Delta_{\mu\nu}, \tag{6}$$

where $\Delta_{\mu\nu} = g_{\mu\nu} - u_\mu u_\nu$ projects any four-vector into the plane orthogonal to u^μ; the metric tensor $g_{\mu\nu} = {\rm diag}(1,-1,-1,-1)$. We also note the invariant scalar entropy density,

$$s = S^\mu\, u_\mu, \tag{7}$$

where the entropy four-current is defined by

$$S^\mu = -\int \frac{{\rm d}^3\boldsymbol{p}}{p_0}\, p^\mu\, [f(x,p)\, \ln f(x,p) - f(x,p)]. \tag{8}$$

In our investigation we will consider the FO process of an ultra-relativistic heavy-ion collision, and the hot region of the fireball shall be deemed to be in chemical ($\mu_\pi = 0$) and local thermal equilibrium $T(x)$. The conserved quantum numbers (*e.g.*, baryon number, electric charge, strangeness) are zero such that the thermal distribution can be characterized by the local temperature parameter $T(x)$ of the fireball. Up to temperatures $T \leq T_{\rm c}$,

most of the particles of such a system are the pions [19,20], which interact via elastic collisions with a cross-section $\sigma_{\pi\pi}^{\text{elastic}}$. Thus, we will consider the invariant scalar functions eqs. (4)–(7) for the case of a Boltzmann gas of pions where only elastic scatterings among the pions are allowed, and moving with a four-flow velocity u^μ. The particle distribution function in such a case is homogeneous $f(x,p) = f(p)$ and given by the Jüttner distribution

$$f_{\text{eq}}(p,T) = g_\pi \, \frac{1}{(2\pi)^3} \, \exp\left(\frac{\mu_\pi - p^\mu u_\mu}{T}\right), \tag{9}$$

where $g_\pi = 3$ is the isospin degeneracy factor and $\mu_\pi = 0$. Since the functions eqs. (4)–(7) are invariant scalars, they can be evaluated in any Lorentz frame. Especially, in the local rest frame RFG we obtain, in the case of a pion gas, characterized by the distribution function (9), the following expressions:

$$n = \frac{g_\pi}{2\,\pi^2} \, m_\pi^2 \, T \, K_2(a), \tag{10}$$

$$e = \frac{g_\pi}{8\,\pi^2} \, m_\pi^3 \, T \, \left[K_1(a) + 3\,K_3(a)\right], \tag{11}$$

$$P = \frac{g_\pi}{2\,\pi^2} \, m_\pi^2 \, T^2 \, K_2(a), \tag{12}$$

$$s = \frac{g_\pi}{2\,\pi^2} \, m_\pi^2 \, \left[T\,K_2(a) + \frac{1}{4}\,m_\pi\,K_1(a) + \frac{3}{4}\,m_\pi\,K_3(a)\right], \tag{13}$$

where $a = m_\pi/T$, and K_n are the Bessel functions of second kind, see appendix A. The Equation of State (EoS) $P(n,T)$ of the pion gas follows from eq. (10) and eq. (12), $P = n\,T$, and the thermodynamical relation $T\,s = e + P$ is also satisfied[1]. In the limit of vanishing pion mass $m_\pi \to 0$ we obtain from eq. (11) and eq. (12) the EoS of an ideal relativistic gas, $e = 3\,P$.

From these considerations we have seen that in RFG the particle density, energy density, entropy density, and pressure are only functions of temperature T. This implies that in any arbitrary Lorentz frame only two thermodynamical unknowns, temperature T and four-flow velocity u_μ, can enter the problem under consideration. To determine both unknowns, we need to have two differential equations, which can be deduced[2] from eq. (3) and eq. (5) [33]:

$$\mathrm{d}u_\mu = \frac{\Delta_{\mu\nu}\,\mathrm{d}T^{\nu\sigma}u_\sigma}{e+P}\,, \tag{15}$$

$$\mathrm{d}e = u_\mu\,\mathrm{d}T^{\mu\nu}\,u_\nu. \tag{16}$$

[1] Recall that a thermodynamical approach by means of the canonical potential of a pion gas,

$$\Omega = g_\pi\,T\int\frac{\mathrm{d}^3\boldsymbol{p}}{(2\pi)^3}\,\ln(1-\exp(-p_0/T)), \tag{14}$$

and with the aid of definitions of energy density $e = -T^2\partial\Omega/\partial T$, pressure $P = -\Omega$ and entropy density $s = \partial\Omega/\partial T$, confirms the findings of eqs. (11)–(13) and the relation $T\,s = e + P$.

[2] For a proof of eq. (15) see footnote 3 in [33], and for eq. (16) see also the remarks in appendix A of [31].

For the left side of eq. (16) we obtain from the scalar invariant (11) the following expression:

$$\mathrm{d}e = \frac{g_\pi}{8\,\pi^2}\,m_\pi^3\,\left[4\,a\,K_0(a) + 8\,K_1(a) + 12\,K_3(a)\right]\,\mathrm{d}T. \tag{17}$$

Equations (15)–(17) can be used to determine the temperature and four-flow velocity, while particle density n, pressure P and entropy density s would follow from their definitions in eqs. (4), (6) and (7), respectively. The differential of the energy momentum tensor needed in eq. (15) and eq. (16) follows from eq. (2),

$$\mathrm{d}T^{\mu\nu} = \int\frac{\mathrm{d}^3\boldsymbol{p}}{p^0}\,p^\mu\,p^\nu\,\mathrm{d}f(x,p)\,, \tag{18}$$

according to which we still need a differential equation for the one-particle distribution function. This will be subject of the next section.

3 Freeze-out process within a finite time-like layer

The scheme of an ultra-relativistic heavy-ion collision can be subdivided into three main stages characterized by their typical temperature parameter T: first, the initial stage at $T_{\text{c}} < T$, where a hot and dense parton gas is produced. Second, the stage at $T_{\text{pre-FO}} \le T \le T_{\text{c}}$ where hadrons are formed. And third, the freeze-out process at temperatures $T_{\text{post-FO}} \le T \le T_{\text{pre-FO}}$ where the hadrons freeze out. After the complete FO of the hadrons at $T = T_{\text{post-FO}}$ the particle interactions cease, *i.e.* the momentum distribution of the particles is frozen out and the hadrons move freely towards the detector.

In this section we are concerned with the third stage of the collision scheme, *i.e.* we start our investigation of the FO process from the time of the collision where the expanding system reaches a temperature $T = T_{\text{pre-FO}}$ and the hadronization of the primary parton gas is considered to be completed. In the past, the FO process has been usually simulated in two extreme scenarios: a sudden FO on a hypersurface with zero proper thickness $L = 0$, or a gradual FO process during an infinite time and through an infinite space $L \to \infty$.

In this section we present a model for a gradual FO through a finite layer, where the thickness L can be varied from zero to infinity, thus making a bridge between the two extreme schemes mentioned above. Within such a model the FO layer is bounded by two hypersurfaces: the pre-FO hypersurface with $T = T_{\text{pre-FO}}$, where the hydrodynamical description ends, and a post-FO hypersurface with $T = T_{\text{post-FO}}$, where all the matter is frozen out. A covariant model of kinetic FO process within a finite layer has been recently developed, both for the case of space-like [25] and time-like [26] layers; see also [27,28].

In order to get an idea about the physical scales of the total FO time L of the FO layer, we recall that the collision time τ_{coll} between the pions, which are the dominant hadrons, depends on temperature $\tau_{\text{coll}}(T) = 12\,f_\pi^4/T^5$ [34–36], where $f_\pi = 92.4\,\text{MeV}$ is the pion decay constant

($1 = 0.19733\,\mathrm{GeV\,fm}$). At the pre-FO side of the layer there is a temperature of $T_{\text{pre-FO}} \approx 175\,\mathrm{MeV}$ and the collision time is small: $\tau_{\text{coll}} \simeq 1.1\,\mathrm{fm}/c$. The proper thickness L (in time) of the FO layer is taken typically of the order of a few (at least one) collision time $\tau_{\text{coll}}(T)$ at $T = T_{\text{pre-FO}} \sim T_{\text{c}}$, *i.e.* $L \sim (5\text{–}10)\,\mathrm{fm}/c$.

Here, we will not repeat the theoretical developments of [25–28] in detail, but should consider the essential steps relevant for our investigations.

To describe the gradual FO process, the one-particle distribution function is decomposed into two components, an interacting part f_i and a frozen-out part f_f,

$$f(x,p) = f_i(x,p) + f_f(x,p). \tag{19}$$

During the FO process the number of interacting particles decreases from the pre-FO to the post-FO side, where by definition the number of interacting particles tends to zero. As boundary conditions we assume on the pre-FO side of the layer a thermal equilibrium, *i.e.* a Jüttner distribution (9) for f_i and $f_f = 0$, while on the post-FO side f_i vanishes; for an illustration see also fig. 1 in [25].

The space-time evolution of the interacting and non-interacting components during the FO should be modeled by the Boltzmann Transport Equation (BTE). We will use the relaxation time approximation and apply the escape rate $P_{\text{esc}}(x,p)$, describing the escape of particles from the interacting component f_i to the non-interacting component f_f. The FO is a strongly directed process, *i.e.* the gradient in one preferred FO direction, $\mathrm{d}\sigma_\mu = (\mathrm{d}\sigma_0, \mathrm{d}\boldsymbol{\sigma})$, is much stronger than the changes in the perpendicular directions, thus we can neglect these FO gradients in the perpendicular directions. Then, the BTE can be transformed into the following differential equations [25–28]:

$$\begin{aligned}\mathrm{d}\sigma^\mu\,\partial_\mu f_i(x,p) &= -P_{\text{esc}}(x,p)\,f_i(x,p)\\ &\quad + \frac{1}{\tau_{\text{th}}}[f_{\text{eq}}(p) - f_i(x,p)],\end{aligned} \tag{20}$$

$$\mathrm{d}\sigma^\mu\,\partial_\mu f_f(x,p) = P_{\text{esc}}(x,p)\,f_i(x,p)^3. \tag{21}$$

Here, $p_\mu = (p_0, \boldsymbol{p})$ is the four-momentum of the particle, and $x_\mu = (t, \boldsymbol{r})$ is the four-coordinate of the particle. The second term in eq. (20) is the re-thermalization term (see below), which describes how fast the system relaxes into some thermalized distribution function f_{eq} during a characteristic time scale τ_{th}.

A Lorentz-invariant expression for the escape rate is given by [24–28]:

$$P_{\text{esc}}(x,p) = \frac{1}{\tau_0}\frac{L}{L - x^\mu\,\mathrm{d}\sigma_\mu}\,\frac{p^\mu\,\mathrm{d}\sigma_\mu}{p^\mu\,u_\mu}\,\Theta(p^\mu \mathrm{d}\sigma_\mu)\,, \tag{23}$$

where τ_0 is the characteristic FO time. The Θ-function is the Bugaev cut-off factor [37], which is important only for the FO in the space-like direction.

We have to insert the escape rate P_{esc} into eqs. (20) and (21). In the following we will consider the FO process of a pion gas through a finite layer with a time-like normal $\mathrm{d}\sigma_\mu\,\mathrm{d}\sigma^\mu = +1$, so that L becomes a thickness in time. We will work in the rest frame of the FO front (RFF) where $\mathrm{d}\sigma_\mu = (1,0,0,0)$. Thus, we obtain the following set of differential equations:

$$\partial_t f_i = -\frac{1}{\tau_0}\left(\frac{L}{L-t}\right)\left(\frac{p^0}{p_\mu\,u^\mu}\right) f_i + \frac{1}{\tau_{\text{th}}}[f_{\text{eq}}(p) - f_i], \tag{24}$$

$$\partial_t f_f = +\frac{1}{\tau_0}\left(\frac{L}{L-t}\right)\left(\frac{p^0}{p_\mu\,u^\mu}\right) f_i. \tag{25}$$

Note again, the first term in eqs. (24) and (25) describes the transition of the pions from the interacting to the frozen-out component. The second term in eq. (24) is the re-thermalization term [33,38] which describes how the interacting component relaxes to some thermal distribution f_{eq}, where the parameters of it, $T(t)$, $u_\mu(t)$, have to be calculated from the conservation laws. The strength of both terms is characterized by their typical time scales, the characteristic freeze-out time τ_0 and the relaxation time τ_{th}, respectively [26,33,38–41].

In the case of fast re-thermalization $\tau_{\text{th}} \ll \tau_0$, the interacting component can be choosen as equilibrated Jüttner distribution for all the times [25]. Then, we obtain, with the aid of eq. (18), for the energy momentum tensor of the interacting component

$$\begin{aligned}\frac{\mathrm{d}T_i^{\mu\nu}}{\mathrm{d}t} &= \int \frac{\mathrm{d}^3\boldsymbol{p}}{p^0}\,p^\mu\,p^\nu\,\partial_t\,f_i(x,p)\\ &= -\frac{1}{\tau_0}\left(\frac{L}{L-t}\right)\int \frac{\mathrm{d}^3\boldsymbol{p}}{p^0}\,p^\mu\,p^\nu\,\left(\frac{p^0}{p_\mu\,u^\mu}\right)\\ &\quad \times f_{\text{eq}}(p, T(t), u_\mu(t)).\end{aligned} \tag{26}$$

In the following we will give the components of eq. (26) in the RFF, where $u^\mu_{\text{RFF}} = \gamma(1,v,0,0)$ with $\gamma = 1/\sqrt{1-v^2}$:

$$\frac{\mathrm{d}T_i^{00}(t,v,T,m_\pi)}{\mathrm{d}t} = \frac{1}{\tau_0}\frac{L}{L-t}\frac{nT}{4}\frac{1}{\gamma\,v}\left(G_2^-(m_\pi,v,T) - G_2^+(m_\pi,v,T)\right)\,, \tag{27}$$

$$\begin{aligned}\frac{\mathrm{d}T_i^{0x}(t,v,T,m_\pi)}{\mathrm{d}t} &= \frac{1}{v}\frac{\mathrm{d}T_i^{00}(t,v,T,m_\pi)}{\mathrm{d}t}\\ &+ \frac{1}{\tau_0}\frac{L}{L-t}\frac{nT}{2}\frac{b^2}{\gamma\,v}\left((3+v^2)K_2(a) + a\,K_1(a)\right),\end{aligned} \tag{28}$$

$$\begin{aligned}\frac{\mathrm{d}T_i^{xx}(t,v,T,m_\pi)}{\mathrm{d}t} &= \frac{1}{v}\frac{\mathrm{d}T_i^{0x}(t,v,T,m_\pi)}{\mathrm{d}t}\\ &- \frac{T}{\gamma\,v}\left(\frac{\mathrm{d}N_i^x(t,v,T,m_\pi)}{\mathrm{d}t} - \frac{1}{v}\frac{\mathrm{d}N_i^0(t,v,T,m_\pi)}{\mathrm{d}t}\right)\\ &+ \frac{1}{\tau_0}\frac{L}{L-t}\frac{nT}{2}a\,b\left(\frac{1}{v^2}(1+3v^2)K_2(a) + b\,K_1(a)\right),\end{aligned} \tag{29}$$

[3] Troughout the paper we shall use the notation

$$\partial_\mu\,f(x,p) \equiv \frac{\partial}{\partial x^\mu}\,f(x,p), \tag{22}$$

i.e. expressions like (22) are not infinitesimal quantities. Note, the finite normal vector on the hypersurface is normalized by $\mathrm{d}\sigma_\mu\,\mathrm{d}\sigma^\mu = \pm 1$ where the upper sign is for the time-like and the lower sign is for the space-like normal, respectively; note that $\mathrm{d}\sigma_\mu$ is also not an infinitesimal quantity but a finite vector (an explicit expression for the time-like normal is given below).

and the needed components of time derivative of the particle four-current are given by

$$\frac{\mathrm{d}N_i^0(t,v,T,m_\pi)}{\mathrm{d}t} = \frac{1}{\tau_0}\frac{L}{L-t}\frac{n}{4}\left(G_1^-(m_\pi,v,T) - G_1^+(m_\pi,v,T)\right), \tag{30}$$

$$\frac{\mathrm{d}N_i^x(t,v,T,m_\pi)}{\mathrm{d}t} = \frac{1}{v}\frac{\mathrm{d}N^0(t,v,T,m_\pi)}{\mathrm{d}t} + \frac{1}{\tau_0}\frac{L}{L-t}\frac{n}{4}\left(\frac{4aK_1(a)}{v} + \frac{2a^2K_0(a)}{v}\right), \tag{31}$$

where we recall that $a = m_\pi/T$ and $b = \gamma\, a$; the functions $G_n^\pm$ and K_n are defined in appendix A. According to these expressions we also need the invariant scalar pion density n defined in eq. (4), and according to eq. (15) we also need the pressure P defined in eq. (6). Since they are invariant scalars, we can take the explicit expressions given in eq. (10) and eq. (12) evaluated in the RFG for a Jüttner distribution. By inserting these results and eqs. (27)–(29) into eq. (15) and eq. (16), we obtain a set of two differential equations for the two unknowns T and v. Taking $u^\mu_{\mathrm{RFF}} = \gamma(1,v,0,0)$, $u_\mu^{\mathrm{RFF}} = \gamma(1,-v,0,0)$, $\mathrm{d}u_0^{\mathrm{RFF}} = \gamma^3\, v\,\mathrm{d}v$ and $\mathrm{d}u_x^{\mathrm{RFF}} = -\gamma^3\,\mathrm{d}v$, we obtain explicitly in RFF:

$$\frac{\mathrm{d}T}{\mathrm{d}t} = \frac{8\,\pi^2}{g_\pi\, m_\pi^3}\left(4\,a\,K_0(a) + 8K_1(a) + 12K_3(a)\right)^{-1}\,\gamma^2 \times\left(\frac{\mathrm{d}T_i^{00}}{\mathrm{d}t} - 2v\frac{\mathrm{d}T_i^{0x}}{\mathrm{d}t} + v^2\frac{\mathrm{d}T_i^{xx}}{\mathrm{d}t}\right), \tag{32}$$

$$\frac{\mathrm{d}v}{\mathrm{d}t} = \frac{2\pi^2}{g_\pi\, m_\pi^3\, T}\left(\frac{1}{4}K_1(a) + \frac{3}{4}K_3(a) + \frac{1}{a}K_2(a)\right)^{-1} \times\left(-v\frac{\mathrm{d}T_i^{00}}{\mathrm{d}t} + (1+v^2)\frac{\mathrm{d}T_i^{0x}}{\mathrm{d}t} - v\frac{\mathrm{d}T_i^{xx}}{\mathrm{d}t}\right). \tag{33}$$

Notice, that the degeneracy factor g_π is actually cancelled against the same factor contained in the scalar particle density n of energy momentum components, see eq. (10). In the limit of vanishing pion mass $m_\pi \to 0$ the eqs. (32) and (33) simplify to

$$\frac{\mathrm{d}T}{\mathrm{d}t} = -\frac{1}{\tau_0}\,\frac{L}{L-t}\,\frac{1}{4}\,T\,\gamma\,, \tag{34}$$

$$\frac{\mathrm{d}v}{\mathrm{d}t} = -\frac{1}{\tau_0}\,\frac{L}{L-t}\,\frac{1}{4}\,\frac{v}{\gamma}\,, \tag{35}$$

in agreement with the corresponding limit given in eq. (9) in [26][4]. The system of the two differential equations (32), (33), together with the invariant scalars n, e, P in eqs. (10)–(12) and the components of the energy momentum tensor given in eqs. (27)–(29) constitute a closed set of equations for the unknowns $T(t)$ and $v(t)$ inside the FO layer. Once these both unknows have been determined self-consistently, all other quantities like the particle density $n(t)$, the pressure $P(t)$ and the entropy density $s(t)$ inside the finite layer can be determined by their expressions given in eqs. (10)–(13).

In our investigation, we are interested on the impact of in-medium pion mass modification on the FO process. Therefore, we have to implement a temperature-dependent pion mass $m_\pi(T)$ in the given equations. The results of such an investigation can then be compared with the corresponding findings where a vacuum pion mass m_π or massless pions are implemented[5].

4 Pion mass shift at finite temperature

Typical conditions inside the FO layer are high temperatures, typically between $100\,\mathrm{MeV} \le T \le 175\,\mathrm{MeV}$. Such extreme conditions imply a strong modifications of the hadrons in respect to their mass, coupling constants and decay rates are expected. One aim of our investigation is to evaluate how strong the impact of the pion mass shift on the kinetic FO process of a pion gas is. The kinetic FO process of a pion gas concerns elastic interactions among these particles and how these elastic scatterings cease. Therefore, we have to determine the mass modification of pions embedded in a pion gas with elastic scatterings among these particles. However, the impact of non-elastic interactions on the mass modification of pions becomes relevant for a description of the chemical FO process.

4.1 Pion mass in vacuum

First, let us briefly re-consider the mass of a pion in vacuum, defined as pole mass of the pion propagator:

$$\Pi_\pi^a(p) = i\int \mathrm{d}^4x\,\mathrm{e}^{ipx}\,\langle \mathrm{T_W}\,\hat{\Phi}^a(x)\hat{\Phi}^{a\,\dagger}(0)\rangle_0 = \frac{1}{p^2 - \overset{\circ}{m}{}_\pi^2 - \Sigma_\pi^a(p) + i\epsilon}\,, \tag{38}$$

where $\langle\hat{\mathcal{O}}\rangle_0 = \langle 0|\mathcal{O}|0\rangle$ is the vacuum expectation value of an operator $\hat{\mathcal{O}}$, $a = 1, 2, 3$ is the isospin index, $\mathrm{T_W}$ is the

[4] Note that in the case of a massless pion gas we have, due to Jüttner distribution,

$$e = g_\pi\,\frac{4\,\pi}{(2\pi)^3}\int_0^\infty \mathrm{d}p\,p^3\,\exp(-p/T) = 3\,g_\pi\,T^4/\pi^2, \tag{36}$$

while in [26] a Bose gas was assumed for the EoS:

$$e_{\mathrm{Bose}} = g_\pi\,\frac{4\,\pi}{(2\pi)^3}\int_0^\infty \mathrm{d}p\,p^3\,\left[\exp(p/T) - 1\right]^{-1} = g_\pi\,\pi^2\,T^4/30. \tag{37}$$

The difference is only marginal. However, in eq. (9) of ref. [26] we have actually to imply the relation $n_{\mathrm{Bose}} = e_{\mathrm{Bose}}/(3\,T) = g_\pi\,\pi^2\,T^3/90$ valid for massless pions, to get the agreement stated above.

[5] We note, however, that the in-medium modified pion mass not only changes slightly the distribution function, but also the pionic EoS and correspondingly the expansion dynamics, *e.g.* [42]. We note, that such a consideration could also be investigated, within the expanding model very recently developed in [43].

Wick time ordering, $\hat{\Phi}^a$ is the second-quantized pion field operator and Σ_π^a is the self-energy of pion a in vacuum. The parameter $\overset{\circ}{m}_\pi$ is the so-called bare pion mass which enters the Lagrangian of the effective hadron model of QCD. The physical pion mass is defined as the pole of propagator, eq. (38), *i.e.* as the self-consistent solution of

$$m_\pi^2 = \overset{\circ}{m}{}_\pi^2 + \mathrm{Re}\,\Sigma_\pi(p^2 = m_\pi^2). \tag{39}$$

The vacuum pion mass is $m_\pi^0 = 135.04\,\mathrm{MeV}$, $m_\pi^\pm = 139.63\,\mathrm{MeV}$. Despite the enormous effort in the quantum field theory, a rigorous derivation of the vacuum pion mass from first principles of QCD has not been found so far. That means the vacuum mass of any hadron cannot be obtained from fundamental QCD without further assumption or new parameters. However, there are promising and sophisticated approaches which have provided some insights into this very involved issue. Among them there are chiral perturbation theory, lattice gauge theory, current algebra, Dyson-Schwinger approach, Nambu-Jona-Lasinio model and QCD sum rules, which provide a link between the quark degrees of freedom of underlaying QCD and the hadronic degrees of freedom. Such approaches allow a derivation of the so-called Gell-Mann–Oakes-Renner (GOR) relation [44,45],

$$m_\pi^2\, f_\pi^2 = -2\, m_q\, \langle \hat{\bar{q}}\hat{q}\rangle_0, \tag{40}$$

which allows to determine the pion mass in vacuum from the microscopic QCD quantities current quark mass m_q and chiral quark condensate at $x = 0$,

$$\langle \hat{\bar{q}}\hat{q}\rangle_0 = \frac{1}{2}\,\langle \hat{\bar{u}}\hat{u} + \hat{\bar{d}}\hat{d}\rangle_0. \tag{41}$$

Typical values are $m_q = (m_u + m_d)/2 = 5.5\,\mathrm{MeV}$, $\langle \hat{\bar{q}}\hat{q}\rangle_0 = -(245\,\mathrm{MeV})^3$; recall, $f_\pi = 92.4\,\mathrm{MeV}$ is the pion decay constant. With these given numerical values, the GOR relation yields $m_\pi = 138\,\mathrm{MeV}$. The pion decay constant can be defined by

$$\langle 0|\hat{A}_\mu^a(0)|\pi^b(q)\rangle = -i\, f_\pi\, q_\mu\, \delta_{ab}, \tag{42}$$

where the isospin indices $a, b = 1, 2, 3$ and

$$\hat{A}_x^a(x) = \hat{\bar{\Psi}}(x)\,\gamma_\mu\,\gamma_5\,\frac{\tau^a}{2}\,\hat{\Psi}(x) \tag{43}$$

is the axial vector current operator, *e.g.* [46]; τ^a are the Pauli spin matrices, and $\hat{\Psi} = (\hat{u}, \hat{d})^{\mathrm{T}}$. From eq. (42) we obtain the expression for the pion decay constant in vacuum,

$$f_\pi = i\,\frac{q^\mu}{q^2}\,\langle 0|\hat{A}_\mu^a(0)|\pi^a(q)\rangle\,, \tag{44}$$

where, due to isospin symmetry, a can be chosen arbitrarily, *e.g.* $a = 3$ (*i.e.* there is no sum over index a). It should be noted that with the aid of LSZ reduction formalism [47,48], the expression (44) can be rewritten as vacuum expectation value over the scalar operator

$$\hat{f}_\pi(0) \equiv i\,\frac{q^\mu}{q^2}\int \mathrm{d}^4y\,\exp(-iqy)\,\left(\Box_y + m_\pi^2\right)\mathrm{T_W}\,\hat{A}_\mu^a(0)\,\hat{\Phi}^{a\,\dagger}(y), \tag{45}$$

that means we basically have

$$f_\pi = \langle \hat{f}_\pi\rangle_0. \tag{46}$$

4.2 Pion mass at finite temperature

Now let us consider the case of pions in-medium. At finite temperature the pions move in a hot and dense bath of hadrons. Accordingly, the in-medium pion propagator reads

$$\begin{aligned}\Pi_\pi^a(p,T) &= i\int \mathrm{d}^4x\,\mathrm{e}^{ipx}\,\langle \mathrm{T_W}\,\hat{\Phi}^a(x)\hat{\Phi}^{a\,\dagger}(0)\rangle_T \\ &= \frac{1}{p^2 - \overset{\circ}{m}{}_\pi^2 - \Sigma_\pi^a(p,T) + i\epsilon}\,.\end{aligned} \tag{47}$$

The thermal Gibbs average $\langle\hat{\mathcal{O}}\rangle_T$ of an operator $\hat{\mathcal{O}}$ is defined by

$$\langle\hat{\mathcal{O}}\rangle_T = \frac{\mathrm{Tr}\langle\hat{O}\,\exp(-\beta\,\hat{H})\rangle}{\mathrm{Tr}\langle\exp(-\beta\,\hat{H})\rangle} = \frac{\sum\limits_{n=0}^{\infty}\langle n|\hat{O}\,\exp(-\beta\,\hat{H})|n\rangle}{\sum\limits_{n=0}^{\infty}\langle n|\exp(-\beta\,\hat{H})|n\rangle}\,, \tag{48}$$

where $\beta = 1/T$. In general, for temperatures $T \geq T_\mathrm{c}$ quark and gluon degrees of freedom would have to be included, *i.e.* the sum in eq. (48) runs in general over quark and gluon eigenstates and over hadron eigenstates of $\hat{H}$. However, in our investigation the temperatures are $T \leq T_\mathrm{c}$, *i.e.* the operator $\hat{H}$ is here an effective Hamiltonian describing the hadron system under consideration. Accordingly, we consider $|n\rangle$ as hadron eigenstates of $\hat{H}$, and the sum runs over the spectrum of all these hadron eigenstates $|n\rangle$. Furthermore, throughout our considerations we are interested on the Gibbs average of operators at $x = 0$, *i.e.* we always have $\langle\hat{\mathcal{O}}\rangle_T = \langle\hat{\mathcal{O}}(x=0)\rangle_T$. As in vacuum, the pion pole mass at finite temperature is defined as the self-consistent solution of

$$m_\pi^2(T) = \overset{\circ}{m}{}_\pi^2 + \mathrm{Re}\,\Sigma_\pi(p^2 = m_\pi^2(T), T). \tag{49}$$

From this equation it becomes obvious why there is an in-medium modification of the pion mass: just because the self-energy $\Sigma_\pi(p,T)$ is now temperature dependent, which changes the position of the pole mass compared to vacuum. Such a change of the pole position is caused by elastic interactions and non-elastic interactions among the particles. To find an expression for the temperature dependence of the pion mass, we will follow a similar way as in vacuum, *i.e.* we will apply the in-medium GOR relation. Especialy, it is a well-known fact that the GOR relation continues to be valid also at finite temperatures, at least up to the order $\mathcal{O}(T^6)$ [49–55]:

$$m_\pi^2(T)\, f_\pi^2(T) = -2\, m_q\, \langle \hat{\bar{q}}\hat{q}\rangle_T\,. \tag{50}$$

We will take relation (50) as a given fact, which would allow a determination of the temperature dependence of the

pion mass; the current quark mass m_q as a fundamental parameter of QCD is of course independent of temperature, while the constituent quark mass M_q is temperature dependent. For that we would have to know the temperature dependence of the chiral condensate and of the pion decay constant. That means, in the generalization of the vacuum expectation values in eqs. (41) and (46), we have now to determine the expressions

$$\langle\hat{\bar{q}}\hat{q}\rangle_T = \frac{\sum\limits_{n=0}^{\infty}\langle n|\hat{\bar{q}}\hat{q}\,\exp(-\beta\,\hat{H})|n\rangle}{\sum\limits_{n=0}^{\infty}\langle n|\exp(-\beta\,\hat{H})|n\rangle}\,, \tag{51}$$

$$f_\pi(T) = \frac{\sum\limits_{n=0}^{\infty}\langle n|\hat{f}_\pi\,\exp(-\beta\,\hat{H})|n\rangle}{\sum\limits_{n=0}^{\infty}\langle n|\exp(-\beta\,\hat{H})|n\rangle}\,, \tag{52}$$

where the operator $\hat{f}_\pi$ is defined in eq. (45). Both of these expressions, $\langle\hat{\bar{q}}\hat{q}\rangle_T$ and $f_\pi(T) = \langle\hat{f}_\pi\rangle_T$, have been evaluated by means of several approaches. The aim is to find an expression both for the chiral condensate and the pion decay constant at finite temperature and consistently within the kinetic model description. Especially, in our approach there are only pions. Accordingly, the Gibbs average of an operator $\hat{\mathcal{O}}$ runs over the diagonal pion states only, *i.e.* $\langle\pi|\hat{\mathcal{O}}|\pi\rangle, \langle\pi\pi|\hat{\mathcal{O}}|\pi\pi\rangle, \ldots$ [56,57], but does not include the diagonal matrix elements of heavier hadrons like kaons, $\langle K^\pm|\hat{\mathcal{O}}|K^\pm\rangle$, etc. Such an approximation can be justified, since at low temperatures $T \leq T_c$, pion states dominate the thermal average, while states containing heavier mesons with a mass $m_n > m_\pi$ are weighted with their corresponding Boltzmann factor $\sim \exp(-m_n/T)$, *i.e.* they are exponentially suppressed [19,20]. For instance, in refs. [19,58] contributions of heavier mesons to the chiral condensate at finite temperature have been studied, where only marginal corrections were found: 5 percent corrections at $T = 100\,\mathrm{MeV}$ and 10 percent corrections at $T = 150\,\mathrm{MeV}$. The Gibbs average (48) can be further approximated by one-pion states [58–60],

$$\langle\hat{\mathcal{O}}\rangle_T = \langle\hat{\mathcal{O}}\rangle_0 + \sum_{n=1}^{3}\int\frac{\mathrm{d}^3p}{(2\pi)^3\,2\,p^0}\,\langle\pi^n(p)|\hat{O}|\pi^n(p)\rangle\exp\left(-\frac{p^0}{T}\right) + \mathcal{O}\left(T^4\right). \tag{53}$$

The contributions of the next higher order $\mathcal{O}(T^4)$ are considered in appendix C, according to which we will neglect multi-pion states in the temperature region considered, see also refs. [56,57]. The pion states are normalized by

$$\langle\pi^n(p_1)|\pi^m(p_2)\rangle = 2\,p_1^0\,(2\pi)^3\,\delta^{(3)}(\boldsymbol{p}_1-\boldsymbol{p}_2)\,\delta_{nm}, \tag{54}$$

with isospin indices $n, m = 1, 2, 3$. With the aid of eq. (53) and according to eqs. (51) and (52), we obtain

$$\langle\hat{\bar{q}}\hat{q}\rangle_T = \langle\hat{\bar{q}}\hat{q}\rangle_0 + \sum_{n=1}^{3}\int\frac{\mathrm{d}^3p}{(2\pi)^3\,2\,p^0}\,\langle\pi^n(p)|\hat{\bar{q}}\hat{q}|\pi^n(p)\rangle\exp\left(-\frac{p^0}{T}\right) + \mathcal{O}\left(T^4\right), \tag{55}$$

$$f_\pi(T) = f_\pi + i\frac{q^\mu}{q^2}\sum_{n=1}^{3}\int\frac{\mathrm{d}^3p}{(2\pi)^3\,2\,p^0}\,\langle\pi^n(p)|\hat{A}^a_\mu|\pi^a(q)\pi^n(p)\rangle \times\exp\left(-\frac{p^0}{T}\right) + \mathcal{O}\left(T^4\right), \tag{56}$$

where in eq. (56) the LSZ reduction of the pion state $\pi^a(q)$ has been transformed back just after the thermal Gibbs average. The pion matrix elements can be determined using the soft-pion theorem [58,61–64] by means of which we obtain (see eqs. (B.5)–(B.8) in appendix B)

$$\langle\hat{\bar{q}}\hat{q}\rangle_T = \langle\hat{\bar{q}}\hat{q}\rangle_0\left(1-\frac{1}{8}\frac{T^2}{f_\pi^2}\,B_1\left(\frac{m_\pi}{T}\right)\right) + \mathcal{O}\left(T^4\right), \tag{57}$$

$$f_\pi(T) = f_\pi\left(1-\frac{1}{12}\frac{T^2}{f_\pi^2}\,B_1\left(\frac{m_\pi}{T}\right)\right) + \mathcal{O}\left(T^4\right), \tag{58}$$

$$m_\pi(T) = m_\pi\left(1+\frac{1}{48}\frac{T^2}{f_\pi^2}\,B_1\left(\frac{m_\pi}{T}\right)\right) + \mathcal{O}\left(T^4\right), \tag{59}$$

for the next higher order $\mathcal{O}(T^4)$ see appendix C. In order to derive relation (59), we have inserted eqs. (57) and (58) into the GOR relation at finite temperature, eq. (50), as well as the GOR in vacuum, eq. (40), has been applied. The function is[6]

$$B_1(z) = \frac{6}{\pi^2}\int_z^\infty \mathrm{d}x\,\sqrt{x^2-z^2}\,\exp(-x) = \frac{6}{\pi^2}\,z\,K_1(z), \qquad \lim_{z\to 0}B_1(z) = \frac{6}{\pi^2}\,. \tag{61}$$

The results (57)–(59) are consistently valid for a pion gas approximated by a Boltzmann gas, *i.e.* with elastic interactions among the pions. Here, we will require the applicability of eqs. (57)–(59) in a temperature region $T \leq T_c$, where the distance between pions is still large[7], and where the correlation between pions is still small [65,66].

According to eq. (59) the pion mass increases with increasing temperature, in line with other theoretical investigations. Especially, more sophisticated approaches yield

[6] In case we would have taken a Bose distribution in eq. (53), then in eqs. (57)–(59) the function B_1 would have to be replaced by the function B_2:

$$B_2(z) = \frac{6}{\pi^2}\int_z^\infty \mathrm{d}x\,\sqrt{x^2-z^2}\,\frac{1}{\exp(x)-1}\,, \quad \lim_{z\to 0}B_2(z) = 1. \tag{60}$$

However, the difference for the pion mass shift using B_1 or B_2 is marginal in the temperature region considered, see fig. 1.

[7] For instance, at $T = 150\,\mathrm{MeV}$ the mean free path of pions is $\lambda \simeq 1/(n\,\sigma_{\pi\pi}^{\mathrm{elastic}}) \simeq 2\,\mathrm{fm}$.

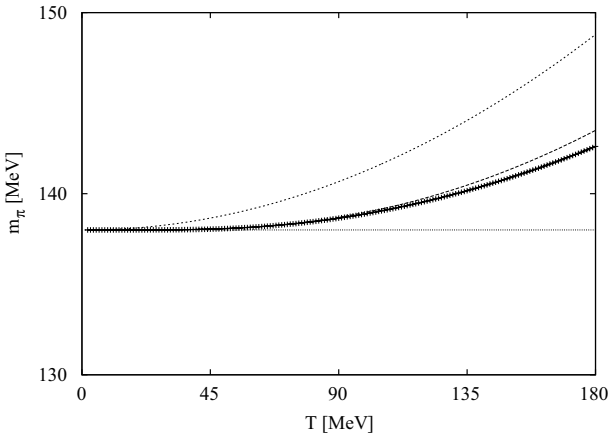

Fig. 1. The temperature-dependent pion mass $m_\pi(T)$: thick solid linepoints show the pion mass for a Boltzmann gas according to eq. (59). The straight dotted line represents a constant pion mass in vacuum, $m_\pi = 138\,\mathrm{MeV}$, according to the GOR relation in vacuum (40). The dashed line represents the pion mass shift in case of a Bose distribution, *i.e.* when in eq. (59) function B_1 is replaced by function B_2. The difference between a pion mass shift of a Boltzmann gas and of a Bose gas are marginal in the temperature region considered. The dotted line (top) represents the result of ChPT according to eq. (64), allowing a comparison of our results with ChPT.

very similar or even the same results for the pion mass shift, *e.g.* chiral perturbation theory (ChPT) [67], Nambu-Jona-Lasinio model [68], QCD sum rules [69,70], linear sigma model [71–74], mean field approximation [75] and virial expansion [76]. For instance, we can compare our findings (57)–(59) with the results of ChPT, since at order $\mathcal{O}(T^2)$ the pions are treated as free particles within ChPT, *e.g.* [77]. For $\langle\hat{\bar{q}}\hat{q}\rangle_T$ [19,78], for $f_\pi(T)$ [77] and for $m_\pi(T)$ [51,77], the ChPT yields the following expressions:

$$\langle\hat{\bar{q}}\hat{q}\rangle_T = \langle\hat{\bar{q}}\hat{q}\rangle_0 \left(1 - \frac{1}{8}\frac{T^2}{f_\pi^2}\right) + \mathcal{O}\left(T^4\right), \tag{62}$$

$$f_\pi(T) = f_\pi \left(1 - \frac{1}{12}\frac{T^2}{f_\pi^2}\right) + \mathcal{O}\left(T^4\right), \tag{63}$$

$$m_\pi(T) = m_\pi \left(1 + \frac{1}{48}\frac{T^2}{f_\pi^2}\right) + \mathcal{O}\left(T^4\right). \tag{64}$$

The difference between our results given in eqs. (57)–(59) and the results of ChPT given in eqs. (62)–(64) simply consists in the function B_1, reflecting the fact that according to the above-mentioned references the ChPT considers a Bose gas and the limit $B_2 \to 1$ (*i.e.* chiral limit $m_\pi \to 0$). The result given in eq. (62) has also been derived in [79] and confirmed later on within the sigma model [80]. The given result in eq. (63) is confirmed, *e.g.* in [56,80–82]. In this respect we should refer the interested reader to ref. [82] where a Páde approximation of $f_\pi(T)$ has been established, valid for arbitrary temperatures $T \leq T_c$. Nonetheless, to apply that result $f_\pi(T)$ one needs a Páde approximation for $\langle\hat{\bar{q}}\hat{q}\rangle_T$ as well in order to be consistent within the entire framework. We also refer to [54,55] where a stronger decrease of the pion decay constant $f_\pi(T)$ and a stronger increase of pion mass $m_\pi(T)$ for high temperatures were found within the framework of Dyson-Schwinger equations.

It is worth mentioning, that for in-medium pion mass shift there is an experimental result available [83–86], namely for the case of a deeply bound pionic state with a π^- at finite baryonic density. Especially, a significant pion mass upshift of $19.3 \pm 2.7\,\mathrm{MeV}$ in ^{207}Pb, *i.e.* approximatly at nuclear saturation density $n_0 \simeq 0.17\,\mathrm{fm}^{-3}$, has been found.

Another important experimental fact concerns the constituent quark number scaling recently found [87,88]. Such a scaling refers to an evident dependence of the hadron elliptic flow v_2 on the number of constituent quarks in the hadron under consideration. This experimental fact can be understood by assuming that FO and pre-hadronization after QGP occurs at an intermediate constituent quark stage [89,90]. Accordingly, the pre-hadrons are made of constituent quarks which have a mass of about $M_q \simeq (200\text{–}300)\,\mathrm{MeV}$. For the pre-pions (this argumentation is not valid for all the other hadrons, because they are considerably heavier than the pions) in QGP it would imply a mass much higher than their vacuum mass $m_\pi \simeq 138\,\mathrm{MeV}$. From this point of view a mass increase with increasing temperature and baryon density is in agreement with these experimental facts. Indeed, QCD sum rules [52] and the QCD Dyson-Schwinger equation [54,55] predict a very strong pion mass up-shift near T_c. In this respect we note that a quark clustering like qq, $q\bar{q}$, gg, qg etc. in the sQGP state has also been proposed in [91,92].

5 Results and discussion

In this section we will present and discuss the solution of the coupled set of differential equations (32) and (33) for massive pions, once with the vacuum pion mass and once with a temperature-dependent pion mass according to eq. (59). In order to ascertain the impact of pion mass itself on the FO process, we will compare these results with the case of massless pions.

The differential equations (32) and (33) are solved with the aid of the Runge-Kutta method [93]. The limit $m_\pi \to 0$ given in eqs. (34) and (35) has been solved independently using MAPLE [94], *i.e.* used as independent verification. The two boundary conditions of these first-order differential equations are the initial temperature on the pre-FO hypersurface, $T_{\text{pre-FO}} \simeq T_c = 175\,\mathrm{MeV}$, and the initial flow velocity on the pre-FO hypersurface of the finite layer, $v_{\text{pre-FO}} = 0.5\,c$. Both of these are typical values; note that such initial temperatures at small baryonic densities can be reached for instance at SPS [95]. In the numerical evaluation we have taken $\tau_0 = 1\,\mathrm{fm}/c$ and $L = 10\,\tau_0$. The results are plotted in figs. 2 and 3.

Let us first consider the temperature of the interacting component plotted in fig. 2. The temperature decreases in time, because the number of interacting particle decreases in time, see also fig. 4. The difference between the case

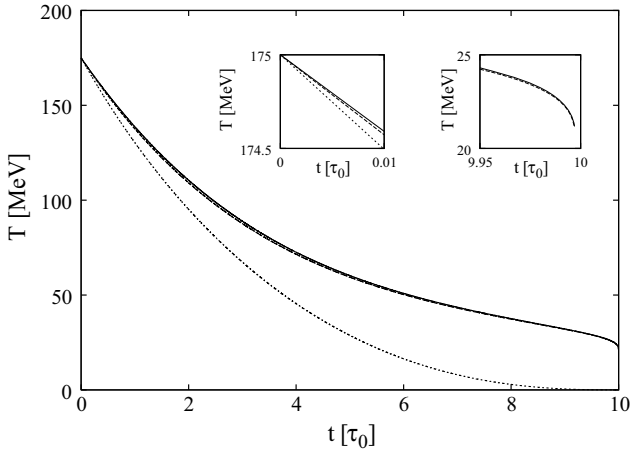

Fig. 2. Temperature of the interacting component as a function of time, when the matter crosses a finite freeze-out layer. In the numerical evaluation we have taken $\tau_0 = 1\,\mathrm{fm}/c$ and $L = 10\,\tau_0$. Three situations of freeze-out are considered: a pion gas with a temperature-dependent pion mass $m_\pi(T)$ (solid line, top), the case of pions with a constant vacuum pion mass m_π (dashed line, middle), and for massless pions $m_\pi = 0$ (dotted line, bottom). As the system expands, the temperature of the interacting component drecreases in all three cases, since the particles with larger momentum freeze out faster. The lighter the pions are, the faster the freeze-out proceeds. In the left inset the marginal impact of the pion mass shift even at extremly high temperatures is shown. The right inset shows the fast drecrease of temperature at the post–freeze-out surface. The substantial difference between the curves for massive pions and massless pions shows how important the impact of the pion mass on the freeze-out process is.

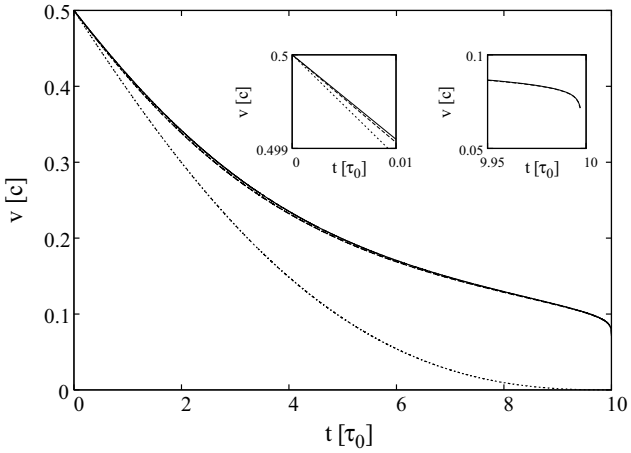

Fig. 3. Velocity of the interacting component as a function of time, when the pions cross a finite freeze-out layer. In the numerical evaluation we have taken $\tau_0 = 1\,\mathrm{fm}/c$ and $L = 10\,\tau_0$. Three cases are considered: massive pions with a temperature-dependent pion mass $m_\pi(T)$ (solid line, top), massive pions with a constant vacuum pion mass m_π (dashed line, middle), and massless pions $m_\pi = 0$ (dotted line, bottom). The line of in-medium modified pion mass (solid line) is above the line of a constant pion mass. This is due to the fact that the pion mass is a bit larger in the former case. During the freeze-out process the fastest particles leave the interacting matter component first, so the velocity of the remaining non-interacting component decreases. The left inset shows the tiny impact of the pion mass shift, while the right inset shows the fast dropping of velocity at the very end of the freeze-out process. The remarkable difference between the curves for massive pions and massless pions shows the importance of pion mass on the freeze-out process.

of a temperature-dependent pion mass $m_\pi(T)$ (solid line) and the case of massive pions with constant vacuum mass m_π (dashed line) is marginal. The reason for that can be understood by means of the left inset of fig. 2: at high temperatures $T \simeq T_\mathrm{c}$ the pion suffers a mass up-shift of about 5 percent of its vacuum mass, see fig. 1. And indeed, at such high temperatures we find a difference of about 5 percent in the temperature slope between the case $m_\pi(T)$ and m_π. However, at such high temperatures the impact of a pion mass is small anyway, because the averaged momentum of pions due to thermal motion is considerably higher than the pion mass itself. At lower temperatures the impact of a pion mass on the FO process is stronger because the averaged momentum of pions becomes comparable with the pion mass itself. However, already at moderate high temperatures of about $T \simeq 135\,\mathrm{MeV}$ the pion mass up-shift is less than 5 percent, see fig. 1, and we cannot expect any longer a significant impact of the mass shift on the FO process. In fact, while the in-medium modification of the pion mass shift has almost no impact, it turns out that there is a significant deviation between the case of massive pions and massless pions. This is due to the fact mentioned, that at moderate high temperatures the pion mass becomes very comparable to the averaged momentum of the pion. In the right small figure implemented in fig. 2 we can see the fast dropping of temperature at the end of the FO process. This is because of the factor $L/(L-t)$ in front of eq. (32) which becomes infinite at the post-FO side of the hypersurface.

Let us now consider the flow velocity of the interacting component plotted in fig. 3. The flow velocity decreases in time, because the number of interacting particles also decreases, see fig. 4. As in the case of temperature, the difference between a FO scenario with a temperature-dependent pion mass $m_\pi(T)$ (solid line) and a constant vacuum pion mass m_π (dashed line) is negligible. The reason for such a behaviour is the very same as in the case of temperature: at the pre-FO side of the layer, there is a remarkable pion mass up-shift of about 5 percent compared to the vacuum pion mass, which implies roughly a 10 percent impact on the flow velocity, as seen in the left inset of fig. 3. However, at such high temperatures $T \simeq T_\mathrm{c}$ the pion mass is considerably smaller than the averaged pion momentum due to thermal motion, so that the impact of a pion mass is negligible. As the system cools down, the pion mass approaches rapidly the vacuum pion mass, see fig. 2. That means, at moderate temperatures of $T \simeq 135\,\mathrm{MeV}$, where a pion mass starts to have some impact on the FO process, the pion mass up-shift is already less than 5 percent, so that the impact of the in-medium modification of the pion mass on the FO process becomes negligible. How-

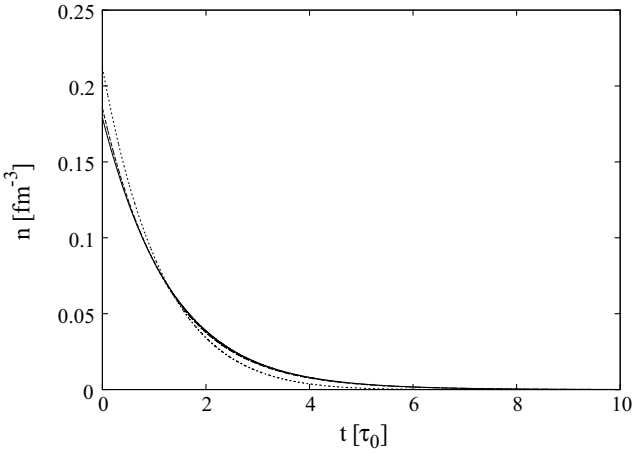

Fig. 4. Density of the interacting component as a function of time, when the pions cross a finite freeze-out layer. In the numerical evaluation we have taken $\tau_0 = 1\,\mathrm{fm}/c$ and $L = 10\,\tau_0$. Three cases are considered: massive pions with a temperature-dependent pion mass $m_\pi(T)$ (solid line), massive pions with a constant vacuum pion mass m_π (dashed line), and massless pions $m_\pi = 0$ (dotted line). During the freeze-out process the particles leave the interacting matter component, so the density of the remaining interacting particles decreases. For the strong decrease of the pion density we recall that for low temperatures the particles decreases exponentially: $\lim_{T\to 0}\, n(T) = g_\pi/(4\pi^2) m_\pi^2\, T\, \sqrt{2\pi/a}\exp(-a)$; $a = m_\pi/T$.

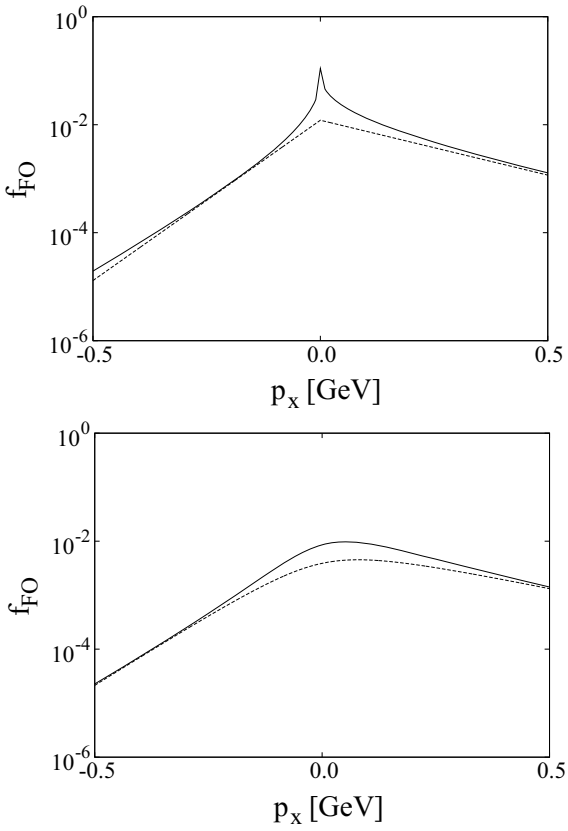

Fig. 5. Top: massless pions. Solid line: FO distribution function $f_{\mathrm{FO}}(p_x) = f_f(t = L, p_x)$, evaluated by means of eq. (25) with $T(t)$ and $v(t)$ evaluated previously, see figs. 2 and 3. Dashed line: a fit of the above solid line by a thermal (*i.e.* Jüttner) distribution with $T = 125\,\mathrm{MeV}$ and $v = 0.49\,c$. Both distribution functions peak sharply. At low momenta p_x, there is a considerable difference between a thermal distribution and the FO distribution function, *i.e.* the FO distribution function $f_{\mathrm{FO}}(p_x)$ evaluated within the kinetic model applied is obviously not a thermal distribution. This is actually one of the main results of the kinetic FO model. Bottom: massive pions. Solid line: FO distribution function $f_{\mathrm{FO}}(p_x) \equiv f_f(t = L, p_x)$ evaluated by means of eq. (25) with $T(t)$ and $v(t)$ evaluated previously, see figs. 2 and 3, and with an in-medium pion mass $m_\pi(T)$. Dashed line: a fit of the above solid line by a thermal Jüttner distribution with $T = 140\,\mathrm{MeV}$ and $v = 0.4\,c$ and $m_\pi(T)$. There is a considerable difference between a thermal distribution and the FO distribution function for a massive pion gas at low momenta p_x, a result which is in agreement with the corresponding statement in the massless case. The distributions for massless and massive pions peak at different momenta p_x! This is expected to effect flow measurements. The sharp peak is smeared out after summing up for fluid elements with different pre-FO flow velocities.

ever, there is a considerable difference between the case of massive pions and massless pions, as can be seen in fig. 3. The right inset implemented in fig. 3 shows that at the post-FO side of the hypersurface the velocity falls down rapidly because of the factor $L/(L - t)$ which becomes infinite at times near L.

Figure 4 shows the rapid decrease of the particle density of the interacting component. More than 90 percent of the particles get frozen out before a time scale of $t \simeq 3\,\tau_0$ is reached, both for the massive and massless case.

In heavy-ion collision experiments the relevant experimental parameters are of course not the temperature $T(t)$ or flow velocity $v(t)$ of the interacting component. Instead, via the experimentally accessible spectrum of the particles $\mathrm{d}N/\mathrm{d}^3p$ one measures the post-FO distribution, which is formed in the applied model at the outer hypersurface, $f_{\mathrm{FO}}(p_x) \equiv f_f(t = L, p_x)$. The Cooper-Frye formula [96]

$$p_0\,\frac{\mathrm{d}N}{\mathrm{d}^3p} = \int_\sigma \mathrm{d}\hat{\sigma}_\mu\, p^\mu\, f_{\mathrm{FO}}(p) = \int \mathrm{d}V\, p_0\, f_{\mathrm{FO}}(p) \sim p_0\, f_{\mathrm{FO}}(p) \qquad (65)$$

allows us to calculate the particle spectrum ($\mathrm{d}\hat{\sigma}_\mu = (\mathrm{d}V, 0, 0, 0)$ is the time-like normal vector of an infinitesimal element of the post-FO hypersurface). In the one-dimensional model used, the volume V of the pionic fireball is ill-defined[8], so that only a qualitative comparison with experimental data, for instance the transverse spectrum, is possible, *i.e.* $\frac{\mathrm{d}N}{\mathrm{d}p_x} \sim f_{\mathrm{FO}}(p_x)$, where p_x is locally

[8] Since the volume of the pionic fireball is not defined, the global energy and momentum conservation cannot be applied. However, global conservation laws can lead to different results if and only if the curvature of the surface is large, thus leading to a significant divergence. Such a situation has been considered in [97], where also related issues concerning an expanding system are discussed.

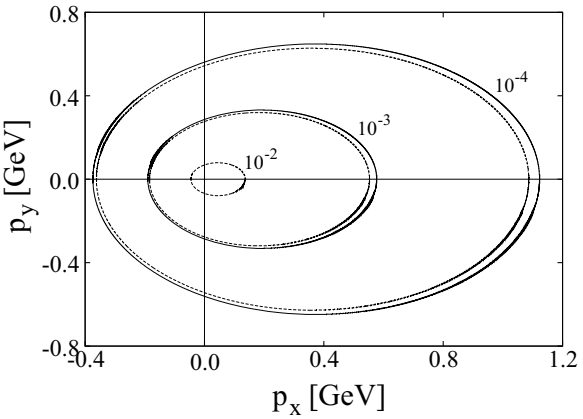

Fig. 6. Contour plot of the FO distribution function, $f_{\rm FO}(p_x, p_y) \equiv f_f(t = L, p_x, p_y)$, evaluated by means of eq. (25) with $T(t)$ and $v(t)$ evaluated previously, see figs. 2 and 3. The solid line is for the case of massive pions $m_\pi(T)$, the dashed line for the case of massless pions. There is no curve for the case of massive pions if $f_{\rm FO} = 10^{-2}$ because the FO distribution function in the case of massive pions is smaller than this value, see fig. 5. It illustrates the importance of pion mass for an accurate FO description. The non-thermal asymmetry of the post-FO particles is a strong and dominant feature, even for a time-like normal FO hypersurface or layer.

pointing out in transverse direction. Due to the marginal impact of in-medium pion mass modification it is meaninful to compare the case of massive pions $m_\pi(T)$ with the case of massless pions, and both of each with a simple thermal distribution.

In fig. 5 the frozen-out distribution functions $f_{\rm FO}(p_x)$ for massless and massive pions are plotted and compared with a thermal distribution. It is shown that at low momenta the distribution function $f_{\rm FO}(p_x)$ evaluated within the kinetic FO model differs considerably from a simple thermal distribution, both for massless and massive pions. This confirms a very recent FO evaluation where a gradual FO with Bjorken expansion and with a constant pion mass $m_\pi = 0.138\,\mathrm{MeV}$ has been considered [43,98]. Notice that the peak position of the distribution function for the case of massive pions differs from the peak position for a massless pion gas. This is expected to effect experimental flow measurements.

In fig. 6 the contour plot $f_{\rm FO}(p_x, p_y)$ for the massive case $m_\pi(T)$ and the massless case $m_\pi = 0$ is compared. For large momenta p there is only a slight difference between the FO of massive and massless pions. However, at low p there is a significant deviation between a massive pion gas and the massless case. Figures 5 and 6 demonstrate that the mass of pions is relevant for an accurate FO description.

6 Summary

The strong interacting quark gluon plasma is not directly accessible via experiments. In fact, one has to trace back from the experimental data to the initially formed new state of matter during an ultra-relativistic heavy-ion collision. This implies a detailed and accurate description of all subsequent stages of the heavy-ion collision process. The kinetic FO process is basically the last stage of the collision after which the particles move freely towards the detectors. Thus, kinetic FO has to be considered as last source of all the observables. Therefore, an accurate description of kinetic FO is compelling for an accurate understanding of the initial stages produced by heavy-ion collisions. Within our FO model of a pion gas described by a Boltzmann gas, we have considered the problem how strong the impact of an in-medium modification of the pion mass on the kinetic freeze-out process is.

We have considered the kinetic FO process through a finite layer for a pion gas with finite pion mass and with massless pions. Throughout the investigation, all calculations have been consistently performed within the model of a pion gas with elastic scatterings among them and approximated by a Boltzmann gas.

First, we have found, that there is a strong impact of the finite pion mass on the FO process compared to a FO process with massless pions. This result is highlighted in figs. 2 and 3, where a significant modification of the basic thermodynamical functions temperature $T(t)$ and flow velocity $v(t)$ of the elastic interacting component of a pion gas inside a finite FO layer has been found.

Hereafter, we have investigated how strong the impact of an in-medium modification of the pion mass on the FO process is. To determine the pion mass at finite temperature, the generalized GOR relation at finite temperature has been applied as a given fact, and the needed expressions $\langle\hat{\bar{q}}\hat{q}\rangle_T$, $f\pi(T)$ have been evaluated by a thermal average over one-pion states. The needed pion matrix elements were evaluated by the soft-pion theorem. Especially, the modification of effective pion mass is increasing with increasing temperature, becoming significant around $100\,\mathrm{MeV}$ and reaches $\simeq 5\,\mathrm{MeV}$ at $T \simeq 180\,\mathrm{MeV}$, see fig. 1.

It has turned out that the impact of the in-medium pion mass shift $m_\pi(T)$ on the FO process is marginal compared to a massive pion gas with a constant pion mass m_π. The physical reason for that can be understood as follows: a significant pion mass shift occurs at high temperatures $T \simeq T_{\rm c}$. However, at such high temperatures the impact of the pion mass itself on the FO process is negligible because the momentum of thermal motion is sizebly larger than the pion mass. During the FO process the temperature decreases rapidly, and after the initial $\sim 2\,\tau_0$ time it was below $T \simeq 100\,\mathrm{MeV}$. But already at moderate temperatures $T \leq 135\,\mathrm{MeV}$, where the impact of the pion mass on the FO process becomes relevant, there is no longer a remarkable in-medium modification of the pion mass.

For a qualitative comparison with experimantal data and in order to investigate the importance of a finite pion mass for the FO process, in figs. 5 the FO distribution function $f_{\rm FO}(p_x)$ has been plotted, both for massive $m_\pi(T)$ and massless $m_\pi = 0$ pions. The FO distribution functions have been compared with a thermal distribution. It is shown that at low momenta there is a considerable difference to a thermal spectrum, both for a massive and

massless pion gas. The distributions peak at different momenta p_x, which is expected to affect experimental flow measurements. The contour plot in fig. 6 elucidates a remarkable difference between massive and massless pions at low momenta. Both figs. 5 and 6 show the importance of a finite pion mass for an accurate description of the FO process.

The numerical order of the in-medium pion mass shift at finite temperatures used in our model calculation is in some sense also encouraged from experiments which have found a pion mass up-shift of $19.3 \pm 2.7\,\mathrm{MeV}$ around the baryon saturation density $n_0 \simeq 0.17\,\mathrm{fm}^{-3}$ [83–86]. However, we have to take into account that the in-medium pion mass shift might be much more pronounced at high temperatures $T \simeq T_\mathrm{c}$ than at those used in our model calculations. For instance, QCD sum rules [52] and QCD Dyson-Schwinger equation [54,55] predict a strong pion mass up-shift near T_c.

Such a strong in-medium modification of the pion mass would be also in line with the argumentation of quark pre-clustering inside the QGP for temperatures higher but near the QCD phase transition at $T \geq T_\mathrm{c}$, because the quarks will have a constituent quark mass of about $M_q \simeq 200$–$300\,\mathrm{MeV}$, so that the mass of pre-pions for such temperature regions would be much higher than the vacuum pion mass. Our results indicate that an earlier pre-hadronization and FO at higher temperatures would increase the sensitivity on the changing of effective pion mass.

From the experimental side, as mentioned in sect. 4, such a conclusion is mainly supported by the experimental fact of the constituent quark number scaling, *i.e.* the dependence of the hadron elliptic flow v_2 on the number of constituent quarks of the hadrons. Therefore, for a more comprehensive analysis on how strong the impact of an in-medium modification of the pion mass for an accurate description of a heavy-ion collision process is, further insides of (pre-)pion mass shift near (and beyond) the critical temperature T_c, both from theoretical as well as experimental side, are mandatory. Especially, the pion mass modification caused by non-elastic scatterings among the pions have to be evaluated in order to describe the chemical FO process.

In summary, in our model study we come to the conclusion that, while a pion mass m_π has a significant impact on the kinetic FO process, the temperature dependence of the pion mass $m_\pi(T)$ is negligible for an accurate description of the kinetic FO process.

S.Z. thanks for the pleasant hospitality at the Bergen Center for Computational Science (BCCS) and Bergen Center Physics Laboratory (BCPL) at the University of Bergen/Norway. Kalliopi Kanaki is acknowledged for giving valuable information and suggestions. The authors acknowledge detailed and fruitful discussions with Volodymyr Magas. Dag Toppe Larsen, Magne Håvåg and Miklos Zetenyi are acknowledged for their computer assistance. Sincere thanks to Fred Kurtz for a critical reading of the manuscript.

Appendix A.

The function $G_n^\pm$ $(n = 1, 2)$ is defined by

$$G_n^\pm(m_\pi, v, T) = \frac{1}{T^{n+2}} \int_0^\infty \mathrm{d}p\, p \left(\sqrt{p^2 + m_\pi^2}\right)^n \times \mathrm{E}_1\left(\frac{\gamma}{T}\sqrt{p^2 + m_\pi^2} \pm \frac{\gamma\, v\, p}{T}\right), \tag{A.1}$$

where E_1 is a special case of incomplete Gamma-function [99]

$$\mathrm{E}_1(x) = \int_x^\infty \mathrm{d}t\, t^{-1}\, \mathrm{e}^{-t}. \tag{A.2}$$

In the massless case we get the temperature-independent limits

$$\lim_{m_\pi \to 0} G_1^\pm = \frac{2}{3}\frac{1}{\gamma^3}\frac{1}{(1 \pm v)^3}, \qquad \lim_{m_\pi \to 0} G_2^\pm = \frac{3}{2}\frac{1}{\gamma^4}\frac{1}{(1 \pm v)^4}. \tag{A.3}$$

The function K_n is the Bessel function of second kind [99], defined by

$$K_n(z) = \frac{2^n\, n!}{(2n)!} z^{-n} \int_z^\infty \mathrm{d}x\, \mathrm{e}^{-x}\, (x^2 - z^2)^{n-1/2}. \tag{A.4}$$

Appendix B.

In this appendix we will evaluate the matrix elements in eqs. (55) and (56) with the aid of the soft-pion theorem [58,61–64] (a derivation of the soft-pion theorem for the here-used simplier case of "free" pions can be found in the appendix of ref. [100]) given by

$$\lim_{p_2 \to 0} \lim_{p_1 \to 0} \langle \pi^m(p_2) | \hat{\mathcal{O}}(x) | \pi^n(p_1) \rangle = \frac{1}{f_\pi^2} \langle 0 | \left[\hat{Q}_A^m, \left[\hat{\mathcal{O}}(x), \hat{Q}_A^{n\,\dagger} \right]_- \right]_- | 0 \rangle, \tag{B.1}$$

where $\hat{Q}_A^n$ is the (time independent) axial charge, *i.e.* the spatial integral over the zeroth component of the axial vector current (43): $\hat{Q}_A^n = \int \mathrm{d}^3\mathbf{r}\, \hat{A}_0^n(\mathbf{r}, t)$, and $\hat{Q}_A^{n\,\dagger} = \hat{Q}_A^n$; and $n, m = 1, 2, 3$ are the isospin indices. $[\hat{A}, \hat{B}]_- = \hat{A}\hat{B} - \hat{B}\hat{A}$ is the commutator. Here, we are interested in the pion matrix elements of the following two-quark operators at $x = 0$:

$$\hat{\mathcal{O}}_1 = \hat{\bar{q}}\hat{q} \equiv \frac{1}{2}\sum_{i=1}^{3}\sum_{\alpha,\beta=1}^{4} (\gamma_0)_{\alpha\beta} \left(\hat{u}_\alpha^{i\,\dagger}\, \hat{u}_\beta^i + \hat{d}_\alpha^{i\,\dagger}\, \hat{d}_\beta^i \right), \tag{B.2}$$

$$\hat{\mathcal{O}}_2 = \hat{A}_\mu^3 = \frac{1}{2}\left(\hat{\bar{u}}\gamma_\mu\gamma_5\hat{u} - \hat{\bar{d}}\gamma_\mu\,\gamma_5\hat{d} \right) \equiv \frac{1}{2}\sum_{i=1}^{3}\sum_{\alpha,\beta=1}^{4} (\gamma_0\gamma_\mu\gamma_5)_{\alpha\beta} \left(\hat{u}_\alpha^{i\,\dagger}\, \hat{u}_\beta^i - \hat{d}_\alpha^{i\,\dagger}\, \hat{d}_\beta^i \right), \tag{B.3}$$

where the Greek letters α, β denote Dirac indices, μ is the Lorentz index, and i is the color index of quark fields. The equal-time anti-commutators of the full QCD quark fields read for quark operators of the same flavor

$$[\hat{q}^i_\alpha(\mathbf{r}_1,t),\hat{q}^{j\,\dagger}_\beta(\mathbf{r}_2,t)]_+ = \delta^{(3)}(\mathbf{r}_1-\mathbf{r}_2)\,\delta_{\alpha\beta}\,\delta^{i\,j}, \qquad \text{(B.4)}$$

where $[\hat{A},\hat{B}]_+ = \hat{A}\hat{B}+\hat{B}\hat{A}$ is the anti-commutator, while quark fields of different flavor anti-commute. Using identities like $[\hat{A},\hat{B}\hat{C}]_- = [\hat{A},\hat{B}]_+\,\hat{C} - \hat{B}[\hat{A},\hat{C}]_+$ and the anti-commutator relation (B.4) we obtain

$$\lim_{p_2\to 0}\lim_{p_1\to 0}\langle\pi^m(p_2)|\hat{\bar{q}}\hat{q}|\pi^n(p_1)\rangle = -\frac{1}{f_\pi^2}\langle 0|\hat{\bar{q}}\hat{q}|0\rangle\,\delta^{mn}, \quad \text{(B.5)}$$

$$\lim_{p_2\to 0}\lim_{p_1\to 0}\langle\pi^1(p_2)|\hat{A}^3_\mu|\pi^3(q)\pi^1(p_1)\rangle = -\frac{1}{f_\pi^2}\langle 0|\hat{A}^3_\mu|\pi^3(q)\rangle = i\,\frac{1}{f_\pi}\,q_\mu, \quad \text{(B.6)}$$

$$\lim_{p_2\to 0}\lim_{p_1\to 0}\langle\pi^2(p_2)|\hat{A}^3_\mu|\pi^3(q)\pi^2(p_1)\rangle = -\frac{1}{f_\pi^2}\langle 0|\hat{A}^3_\mu|\pi^3(q)\rangle = i\,\frac{1}{f_\pi}\,q_\mu, \quad \text{(B.7)}$$

$$\lim_{p_2\to 0}\lim_{p_1\to 0}\langle\pi^3(p_2)|\hat{A}^3_\mu|\pi^3(q)\pi^3(p_1)\rangle = 0, \qquad \text{(B.8)}$$

where we have also used relation (42).

Appendix C.

In our model we have taken into account the Gibbs average over one-pion states of an operator $\hat{\mathcal{O}}$, see eq. (53). Here we will consider the next order, *i.e.* the Gibbs average over two-pion states of an operator $\hat{\mathcal{O}}$:

$$\mathcal{O}\left(T^4\right) = \frac{1}{2!}\sum_{n,m=1}^{3}\int\frac{\mathrm{d}^3p_1}{(2\pi)^3\,2\,p_1^0}\int\frac{\mathrm{d}^3p_2}{(2\pi)^3\,2\,p_2^0} \times\exp\left(-\frac{p_1^0}{T}\right)\exp\left(-\frac{p_2^0}{T}\right) \times\langle\pi^m(p_2)\pi^n(p_1)|\hat{O}|\pi^n(p_1)\pi^m(p_2)\rangle, \qquad \text{(C.1)}$$

where the factor $(2!)^{-1}$ in front of (C.1) circumvents a double counting by integrating over the permutations $p_1\leftrightarrow p_2$. With the aid of the soft-pion theorem we obtain the pion matrix elements for the chiral condensate and pion decay constant:

$$\sum_{n,m=1}^{3}\lim_{p_2\to 0}\lim_{p_1\to 0}\langle\pi^m(p_2)\pi^n(p_1)|\hat{\bar{q}}\hat{q}|\pi^n(p_1)\pi^m(p_2)\rangle = \frac{9}{f_\pi^4}\,\langle 0|\hat{\bar{q}}\hat{q}|0\rangle, \qquad \text{(C.2)}$$

$$\sum_{n,m=1}^{3}\lim_{p_2\to 0}\lim_{p_1\to 0}\langle\pi^m(p_2)\pi^n(p_1)|\hat{A}^3_\mu|\pi^3(q)\pi^n(p_1)\pi^m(p_2)\rangle = \frac{4}{f_\pi^4}\,\langle 0|\hat{A}^3_\mu|\pi^3(q)\rangle = -i\frac{4}{f_\pi^3}\,q_\mu, \qquad \text{(C.3)}$$

where in eq. (C.3) we have applied eq. (42). By means of these expressions we obtain

$$\langle\hat{\bar{q}}\hat{q}\rangle_T = \langle\hat{\bar{q}}\hat{q}\rangle_0\left(1-\frac{1}{8}\frac{T^2}{f_\pi^2}\,B_1+\frac{1}{128}\frac{T^4}{f_\pi^4}\,B_1^2\right)+\mathcal{O}(T^6), \quad \text{(C.4)}$$

$$f_\pi(T) = f_\pi\left(1-\frac{1}{12}\frac{T^2}{f_\pi^2}\,B_1+\frac{1}{288}\frac{T^4}{f_\pi^4}\,B_1^2\right)+\mathcal{O}(T^6), \quad \text{(C.5)}$$

$$m_\pi(T) = m_\pi\left(1+\frac{1}{48}\frac{T^2}{f_\pi^2}\,B_1+\frac{1}{4608}\frac{T^4}{f_\pi^4}\,B_1^2\right)+\mathcal{O}(T^6), \quad \text{(C.6)}$$

and $B_1\equiv B_1(m_\pi/T)$. A numerical evaluation shows that the terms of order $\mathcal{O}(T^4)$ contribute at most a few percent compared to the terms of order $\mathcal{O}(T^2)$ in the temperature region we are interested in. Within the ChPT approach very similar statements are found, but it should be mentioned that in ChPT non-elastic particle interactions yield additional contributions to order $\mathcal{O}(T^4)$, while eqs. (C.4)–(C.6) are the results for a pion gas with elastic particle collisions only. The dynamical non-elastic interactions among the pions change not only the given numerical values in eqs. (C.4)–(C.6) but also the sign of the coefficients in front of the given order $\mathcal{O}(T^4)$, *e.g.* ref. [57], where the result (C.4) is also mentioned. But we note again that in ChPT the given coefficients of the order $\mathcal{O}(T^2)$ remain untouched even when taking into account the contributions of non-elastic pion scatterings.

Furthermore, in a pion gas with elastic interactions and to all orders in temperature we obtain by iteration

$$\langle\hat{\bar{q}}\hat{q}\rangle_T = \langle\hat{\bar{q}}\hat{q}\rangle_0\left(1-\frac{1}{8}\frac{T^2}{f_\pi^2}+\sum_{n=2}^{\infty}(-1)^n\,\frac{1}{n!}\,\frac{1}{8^n}\,\frac{T^{2n}}{f_\pi^{2n}}\,B_1^n\right), \quad \text{(C.7)}$$

$$f_\pi(T) = f_\pi\left(1-\frac{1}{12}\frac{T^2}{f_\pi^2}+\sum_{n=2}^{\infty}(-1)^n\,\frac{1}{n!}\,\frac{1}{12^n}\,\frac{T^{2n}}{f_\pi^{2n}}\,B_1^n\right), \quad \text{(C.8)}$$

$$m_\pi(T) = m_\pi\left(1+\frac{1}{48}\frac{T^2}{f_\pi^2}+\sum_{n=2}^{\infty}\frac{1}{n!}\,\frac{1}{48^n}\,\frac{T^{2n}}{f_\pi^{2n}}\,B_1^n\right), \quad \text{(C.9)}$$

that means all higher orders are factorial suppressed even at temperatures near T_c. Again we underline that eqs. (C.7)–(C.9) are useful to study the impact of the pion mass shift on the kinetic FO of a pion gas (elastic interactions cease among the pions). However, they are not applicable for modelling the pion mass shift impact on the chemical FO process of a pion gas (non-elastic interactions cease among the pions), because then the non-elastic interactions among the pions will change significantly the given series of higher order.

References

1. CERN Press Release 2000-02-10, `http://press.web.cern.ch/press/PressReleases/`.
2. *Hunting the Quark Gluon Plasma*, BNL Report: BNL-73847-2005, 11th April 2005.

3. BRAHMS Collaboration, Nucl. Phys. A **757**, 1 (2005).
4. PHOBOS Collaboration, Nucl. Phys. A **757**, 28 (2005).
5. STAR Collaboration, Nucl. Phys. A **757**, 102 (2005).
6. PHENIX Collaboration, Nucl. Phys. A **757**, 184 (2005).
7. M. Gyulassy, L. McLerran, Nucl. Phys. A **750**, 30 (2005).
8. E.V. Shuryak, Prog. Part. Nucl. Phys. **53**, 273 (2004).
9. E.V. Shuryak, I. Zahed, Phys. Rev. C **70**, 021901 (R) (2004).
10. E.V. Shuryak, I. Zahed, Phys. Rev. D **69**, 014011 (2004).
11. J.L. Nagle, Eur. Phys. J. C **49**, 275 (2007).
12. F. Karsch, *Lectures on Quark Matter* (Springer, Berlin, 2002) Lect. Notes Phys. **583**, 209 (2002); arXiv: hep-lat/0106019v2.
13. E. Shuryak, Phys. Rev. Lett. **68**, 3270 (1992).
14. T.S. Biró, E. van Doorn, B. Müller, M.H. Thoma, X.-N. Wang, Phys. Rev. C **48**, 1275 (1993).
15. X.N. Wang, Nucl. Phys. A **590**, 47c (1995).
16. K. Geiger, J.I. Kapusta, Phys. Rev. D **47**, 4905 (1993).
17. T. Csörgő, L.P. Csernai, Phys. Lett. B **333**, 494 (1994).
18. L.P. Csernai, I.N. Mishustin, Phys. Rev. Lett. **74**, 5005 (1995).
19. P. Gerber, H. Leutwyler, Nucl. Phys. B **321**, 387 (1989).
20. J. Cleymans, H. Oeschler, K. Redlich, S. Wheaton, Phys. G **32**, 223 (2006).
21. E.L. Bratkovskaya, W. Cassing, C. Greiner, M. Effenberger, U. Mosel, A. Sibirtsev, Nucl. Phys. A **681**, 84 (2001).
22. R. Rapp, J. Wambach, Phys. Lett. B **315**, 220 (1993).
23. V.K. Magas, L.P. Csernai, E. Molnár, A. Nyíri, K. Tamosiunas, Nucl. Phys. A **749**, 202 (2005).
24. L.P. Csernai, V.K. Magas, E. Molnár, A. Nyíri, K. Tamosiunas, Eur. Phys. J. A **25**, 65 (2005).
25. E. Molnár, L.P. Csernai, V.K. Magas, A. Nyíri, K. Tamosiunas, Phys. Rev. C **74**, 024907 (2006).
26. E. Molnár, L.P. Csernai, V.K. Magas, Zs.I. Lázár, A. Nyíri, K. Tamosiunas, J. Phys. G **34**, 1901 (2007).
27. E. Molnár, L.P. Csernai, V.K. Magas, Acta Phys. Hung. A **27**, 359 (2006).
28. V.K. Magas, L.P. Csernai, E. Molnár, Acta Phys. Hung. A **27**, 351 (2006).
29. W. Florkowski, W. Broniowski, Phys. Lett. B **477**, 73 (2000).
30. D. Ziesche, S. Schramm, J. Schaffner-Bielich, H. Stoecker, W. Greiner, Phys. Lett. B **547**, 7 (2002).
31. S. Zschocke, L.P. Csernai, E. Molnár, A. Nyíri, J. Manninen, Phys. Rev. C **72**, 064909 (2005).
32. L.P. Csernai, *Introduction to Relativistic Heavy Ion Collisions* (John Wiley & Sons, Chichester, 1994).
33. Cs. Anderlik, Zs.I. Lázár, V.K. Magas, L.P. Csernai, H. Stöcker, W. Greiner, Phys. Rev. C **59**, 388 (1999).
34. E.V. Shuryak, Phys. Lett. B **207**, 345 (1988).
35. J.L. Goity, H. Leytwyler, Phys. Lett. B **228**, 517 (1989).
36. P. Gerber, H. Leytwyler, J.L. Goity, Phys. Lett. B **246**, 513 (1990).
37. K.A. Bugaev, Nucl. Phys. A **606**, 559 (1996).
38. V.K. Magas, Cs. Anderlik, L.P. Csernai, F. Grassi, W. Greiner, Y. Hama, T. Kodama, Zs. Lázár, H. Stöcker, Phys. Lett. B **459**, 33 (1999).
39. V.K. Magas, C. Anderlik, L.P. Csernai, F. Grassi, W. Greiner, Y. Hama, T. Kodama, Z.I. Lazar, H. Stoecker, Heavy Ion Phys. **9**, 193 (1999).
40. V.K. Magas, Cs. Anderlik, L.P. Csernai, F. Grassi, W. Greiner, Y. Hama, T. Kodama, Zs. Lázár, H. Stöcker, Nucl. Phys. A **661**, 596 (1999).
41. V.K. Magas, A. Anderlik, Cs. Anderlik, L.P. Csernai, Eur. Phys. J. C **30**, 255 (2003).
42. R. Rapp, J. Wambach, Phys. Rev. C **53**, 3057 (1996).
43. V.K. Magas, L.P. Csernai, Phys. Lett. B **663**, 191 (2008).
44. M. Gell-Mann, R.J. Oakes, B. Renner, Phys. Rev. **175**, 2195 (1968).
45. R. Dashen, Phys. Rev. **183**, 1245 (1969); Phys. Rev. D **3**, 1879 (1971).
46. T. Ericson, W. Weise, *Pions and Nuclei* (Oxford Science Publications, Oxford, 1988).
47. H. Lehmann, K. Symanzik, W. Zimmermann, Nuovo Cimento **6**, 319 (1957).
48. C. Itzykson, J.-B. Zuber, *Quantum Field Theory* (McGraw-Hill, New York, 1980).
49. T. Hatsuda, T. Kunihiro, Prog. Theor. Phys. Suppl. **91**, 284 (1987).
50. V. Thorsson, A. Wirzba, Nucl. Phys. A **589**, 633 (1995).
51. R.D. Pisarski, M. Tytgat, Phys. Rev. D **54**, 2989 (R) (1996).
52. C.A. Dominquez, M.S. Fetea, M. Loewe, Phys. Lett. B **387**, 151 (1996).
53. C.L.V. Reyes, PhD Thesis (2005) arXiv: hep-ph/0510124.
54. D. Blaschke, Yu.L. Kalinovsky, P.C. Tandy, arXiv: hep-ph/9811476; *XI. International Conference Problems of Quantum Field Theory, 13th - 17th July 1998, Dubna/Russia*, MPG-VT-UR-169-98, Nov 1998.
55. A. Bender, D. Blaschke, Y. Kalinovsky, C.D. Roberts, Phys. Rev. Lett. **77**, 3724 (1996).
56. M. Dey, V.L. Eletsky, B.L. Ioffe, Phys. Lett. B **252**, 620 (1990).
57. V.L. Eletsky, B.L. Ioffe, Phys. Rev. D **51**, 2371 (1995).
58. T. Hatsuda, Y. Koike, Su H. Lee, Nucl. Phys. B **394**, 221 (1993).
59. A.I. Bochkarev, M.E. Shaposhnikov, Nucl. Phys. B **268**, 220 (1986).
60. V.I. Eletsky, P.J. Ellis, J.I. Kapusta, Phys. Rev. D **47**, 4084 (1993).
61. Y. Nambu, D. Lurie, Phys. Rev. D **125**, 1429 (1962).
62. S.L. Adler, R. Dashen, *Current Algebra and Applications to Particle Physics* (Benjamin, 1968).
63. J.F. Donoghue, E. Golowich, B.R. Holstein, *Dynamics of the Standard Model* (Cambridge University Press, Cambridge, UK, 1992).
64. A. Hosaka, H. Toki, *Quarks, Baryons and Chiral Symmetry* (World Scientific, 2001).
65. H. Leutwyler, A.V. Smilga, Nucl. Phys. B **342**, 387 (1990).
66. V.I. Eletsky, Phys. Lett. B **245**, 229 (1990).
67. T. Inagaki, D. Kimura, A. Kvinikhidze, arXiv: hep-ph/0712.1336.
68. M. Loewe, C. Villavicencio, Phys. Rev. D **67**, 074034 (2003).
69. N. Kodama, M. Oka, Nucl. Phys. A **601**, 304 (1996).
70. C.A. Dominguez, M.S. Fetea, M. Loewe, Phys. Lett. B **387**, 151 (1996).
71. Å. Larsen, Z. Phys. C **33**, 291 (1986).
72. C. Contreras, M. Loewe, Int. J. Mod. Phys. A **5**, 2297 (1990).
73. A. Ayala, S. Sahu, Phys. Rev. D **62**, 056007 (2000).
74. N. Petropoulos, AIP Conf. Proc. **739**, 506 (2005); arXiv: hep-ph/0406258.
75. A. Barducci, R. Casalbuoni, S. De Curtis, R. Gatto, G. Pettini, Phys. Rev. D **46**, 2203 (1992).

76. A. Schenk, Phys. Rev. D **47**, 5138 (1993).
77. J. Gasser, H. Leutwyler, Phys. Lett. B **184**, 83 (1987); **188**, 477 (1987).
78. H. Leutwyler, *Proceedings of the International Conference of High Energy Physics, Uppsala, 1987*, Nucl. Phys. B (Proc. Suppl.) **4**, 248 (1988).
79. V.I. Eletsky, Phys. Lett. B **299**, 111 (1993).
80. A. Bochkarev, J. Kapusta, Phys. Rev. D **54**, 4066 (1996).
81. V.L. Eletsky, Ian I. Kogan, Phys. Rev. D **49**, R3083 (1994).
82. S. Jeon, J. Kapusta, Phys. Rev. D **54**, 6475 (1996).
83. T. Yamazaki, R.S. Hayano, K. Itahashi, K. Oyama, A. Gillitzer, H. Gilg, M. Knülle, M. Münch, P. Kienle, W. Schott, H. Geissel, N. Iwasa, G. Münzenberg, Z. Phys. A **355**, 219 (1996).
84. T. Yamazaki, Nucl. Phys. A **629**, 338c (1998).
85. A. Gillitzer, Nucl. Phys. A **639**, 525c (1998).
86. T. Yamazaki, R.S. Hayano, K. Ithahashi, K. Oyama, A. Gillitzer, H. Gilg, M. Knülle, M. Münch, P. Kienle, W. Schott, W. Weise, H. Geissel, N. Iwasa, G. Münzenberg, S. Hirenzaki, H. Toki, Phys. Lett. B **418**, 246 (1998).
87. PHENIX Collaboration, Phys. Rev. Lett. **91**, 182301 (2003).
88. STAR Collaboration, Phys. Rev. Lett. **92**, 052302 (2004).
89. S.A. Voloshin, J. Phys. Conf. Ser. **9**, 276 (2005).
90. S.A. Voloshin, Nucl. Phys. A **715**, 379 (2003).
91. E.V. Shuryak, I. Zahed, Phys. Rev. D **70**, 054507 (2004).
92. F. Karsch, S. Ejiri, K. Redlich, Nucl. Phys. A **774**, 619 (2006).
93. J.D. Lambert, D. Lambert, *Numerical Methods for Ordinary Differential Systems: The Initial Value Problem* (Wiley, New York, 1991).
94. M. Kofler, *Maple V Release 4* (Addison-Wesley Publishing Company, Bonn, 1996).
95. J. Cleymans, K. Redlich, Phys. Rev. C **60**, 054908 (1999).
96. F. Cooper, G. Frye, Phys. Rev. D **10**, 186 (1974).
97. V.K. Magas, L.P. Csernai, E. Molnar, Eur. Phys. J. A **31**, 854 (2007).
98. V.K. Magas, L.P. Csernai, arXiv: nucl-th/0711.2981.
99. M. Abramowitz, I.A. Stegun, *Handbook of Mathematical Functions* (Dover Publ. Inc., New York, 1970).
100. S. Zschocke, B. Kämpfer, G. Plunien, Phys. Rev. D **72**, 014005 (2005).